

Adjoint-based sensitivity of shock-laden flows

By D. J. Bodony AND A. Fikl†

Shock waves are an essential element of compressible fluids, and they appear in many flows of fundamental and engineering interest. Recent work seeking to understand the sensitivity of shock-laden flows to parametric changes or internal forcing has exposed shortcomings in several of the numerical methods commonly used to compute the adjoint sensitivities. This paper discusses the origin of the shortcomings and identifies the essential properties of a numerical method that yields accurate and well-behaved discrete adjoints. Solution-based stencil upwinding methods, such as weighted essentially non-oscillatory (WENO) or monotonic upstream-centered scheme for conservation laws (MUSCL), do not generate meaningful discrete adjoints, whereas those utilizing localized artificial diffusivity do. Theoretical arguments and numerical examples are used to support this finding.

1. Introduction

The high-speed, high-temperature exhaust of low-bypass-ratio turbofan engines powering tactical carrier-borne naval fighters causes considerable health, communication, and structural issues for crew, aircraft, and ships. Several decades of experimental, theoretical, and computational investigations have identified the basic structure of the jet noise sound sources, with an instability wave/wavepacket concept being the most successful in describing the loudest low-frequency sound radiating toward the aft angles (Suzuki & Colonius 2006; Schlinker *et al.* 2009; Jordan & Colonius 2013).

The exhaust from low-bypass turbofan engines used in naval tactical aircraft is characterized by very high jet exit velocities ($U_j > 1000$ m/s) and high jet exit temperatures ($T_j > 1000$ K), with exact values depending on the engine design and throttle setting (Walton & Burcham 1986). At high afterburner usage, the exit temperatures can exceed 2000 K and the exhaust gas composition differs from that of heated air (Liu *et al.* 2016*a,b*). In addition, the internal nozzle geometry and off-design operating conditions ensure that persistent and strong shock waves will be present within the nozzle and in the exterior flow field, as shown in Figure 1 for a military-style converging-diverging nozzle operating at a total pressure ratio (NPR) of 4.0 and a nozzle total temperature ratio (TTR) of 3.0.

When seeking to understand the sound field generated by the shock-laden jet, or to develop a reduction approach for the noise, using global (Natarajan *et al.* 2018) and/or resolvent mode descriptions of the jet as the basis for noise reduction, the presence of the strong shock waves must be addressed. In prior work, such as that by Kim *et al.* (2014), Natarajan *et al.* (2018), and Karp *et al.* (2020), weak shocks were present but not given specific treatment.

The examination of adjoints in the presence of shocks is surprisingly under-developed, despite the use of adjoint-based optimization for aerodynamic flows with shocks (Jameison 1988). The analytical study of the steady quasi-one-dimensional Euler equations by

† Department of Aerospace Engineering, University of Illinois at Urbana-Champaign

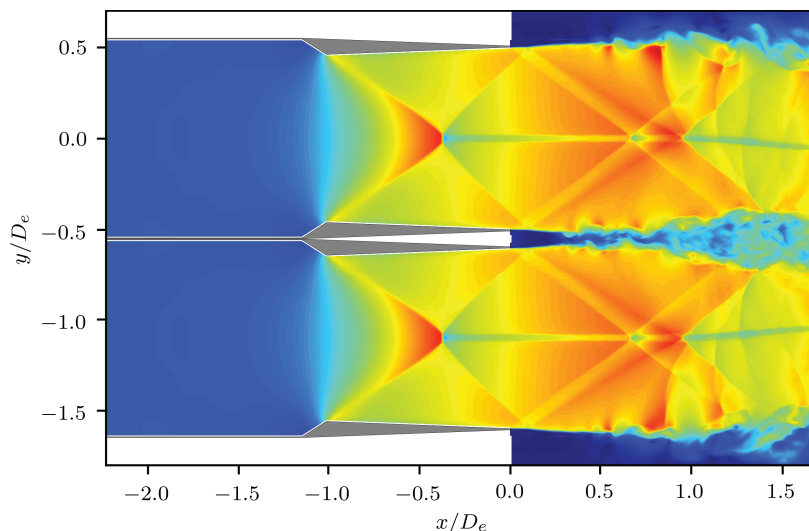


FIGURE 1. Sample flow field from a twin military-style converging-diverging nozzle with NPR = 4.0 and TTR = 3.0. Observe the persistent normal and oblique shocks within and external to the nozzle.

Giles & Pierce (2001), for example, shows that by good fortune the adjoint variables for these equations have a zero gradient at a normal shock, as a consequence of the specific objective function chosen and the Rankine-Hugoniot jump condition, and an internal boundary condition of the adjoint field at the shock location. It is not known how the oblique or unsteady shocks influence the adjoint field, nor has there been a study of how forward and adjoint global and/or resolvent modes are affected by a shock.

In contrast, the solutions of the adjoint equations in the presence of shocks may converge when the artificial dissipation is scaled to increasingly smear out the shock as the grid is refined (Giles & Ulbrich 2010*a,b*). For example, in a finite-volume context with a Lax-Friedrich scheme applied to the inviscid Burgers equation, the artificial dissipation μ in

$$F_{i+1/2} = \frac{1}{2}(f_{i+1} + f_i) - \mu(u_{i+1} - u_i)$$

must vary as $\mu = (\Delta x)^\alpha$, for $\alpha \in (2/3, 1)$, for a discrete adjoint to converge. Under these conditions the shock is spread over an increasing number of grid points as $\Delta x \rightarrow 0$, in contradistinction to the usual desire for a resolved flow field to sharpen as the grid is refined.

In very recent work, Cook & Nichols (2022) use a linearized kinematic shock boundary condition and shock-aligned grids to estimate the sensitivities generated by a curved shock to free stream disturbances. Their work does not address the adjoint-based sensitivities of concern here and relies on knowledge of a single, steady shock. It is not clear how their method would generalize to the flow field of Figure 1.

The premise of this paper is to examine the interplay between numerics and the need to compute the sensitivity of one or more measures of the flow when shocks are present. This goal is explored in the context of the inviscid limit of Burgers equation for which analytical results serve as a guide.

2. Forward and adjoint analytical solutions of Burgers equation with shocks

We will focus on the Riemann problem for the inviscid Burgers equation, written as

$$u_t + f(u)_x = 0 \quad \text{for } t \in (0, T] \text{ and } a < x < b, \quad (2.1)$$

$$u(x, 0) = u_L H(x_0 - x) + u_R H(x - x_0), \quad (2.2)$$

where $H(x)$ is the Heaviside function and $f(u) = u^2/2$ is the convex flux function. We further assume that $\text{sgn} \llbracket u \rrbracket = -\text{sgn} \{\{u\}\}$ so that a shock originates from $x = x_0$ and travels with velocity $s = \llbracket f(u) \rrbracket / \llbracket u \rrbracket = \{\{u\}\}$, where $\llbracket u \rrbracket = u_R - u_L$ and $\{\{u\}\} = (u_L + u_R)/2$. We introduce the adjoint $p(x, t)$ by first defining an objective function

$$\mathcal{J}[u] = \frac{1/2}{b-a} \int_a^b (u(x, T) - u^*(x))^2 dx = \int_a^b G(u) dx \quad (2.3)$$

to measure the difference between the final solution $u(x, T)$ and a desired field $u^*(x)$. By following the standard calculus of variations procedure and noting that the solution has a jump at location $x_s(T) = x_0 + st$, it can be shown that the adjoint field satisfies

$$-p_t - up_x = 0, \quad \text{for } t \in [0, T] \text{ and } x \in [a, x_s^-(t)] \cup (x_s^+(t), b], \quad (2.4)$$

$$p(x, T) = G'(u(x, T)), \quad (2.5)$$

$$p(t, x_s(t)) = y_s(t), \quad (2.6)$$

where $y_s(t)$ is an internal boundary condition given by

$$-\llbracket u \rrbracket \dot{y}_s = 0, \quad (2.7)$$

$$y_s(T) = \llbracket G(u(x_s(T), T)) \rrbracket / \llbracket u(x_s(T), T) \rrbracket, \quad (2.8)$$

and where the integration in time is from $t = T$ to $t = 0$. There are two key features of the adjoint system. The first is that both the advection velocity $u(x, T)$ and the initial condition $p(x, T)$ have a discontinuity at $x = x_s(T)$. The hypersingularity of the adjoint problem leads to ill-posedness concerns that are resolved with the vanishing viscosity solution (Bouchut & James 1998). In other words, the adjoint is unique only when the shock creation process is explicitly considered, implying that the ability of the discrete adjoint of any numerical method used to solve the forward problem is not guaranteed to correctly solve the adjoint problem. A second key feature is that the shock becomes an internal boundary condition in the adjoint problem.

3. Forward and adjoint numerical methods and solutions for Burgers' equation

To solve the inviscid Burgers' equation numerically with a shock in the initial condition, we appeal only to those numerical methods suitable for approximating discontinuous solutions, based either on finite volume concepts (Leveque 2002), WENO (Jiang & Shu 1996) or on artificial viscosity methods (Kawai & Lele 2008). It is a convenient fact that each of these numerical methods can be expressed in the method-of-lines form of

$$\frac{d\mathbf{u}}{dt} + \mathbf{D}_1[\mathbf{u}]\mathbf{f} = \mathbf{P}^{-1}\tilde{\mathbf{D}}_p^T\Phi[\mathbf{u}]\tilde{\mathbf{D}}_p\mathbf{u} + \text{BC}, \quad (3.1)$$

where $\mathbf{D}_1 = \mathbf{P}^{-1}\mathbf{Q}$ is a first derivative operator, possibly dependent on the solution \mathbf{u} (as in WENO), $\Phi[\mathbf{u}]$ is an artificial dissipation or upwinding term that is dependent on the solution \mathbf{u} , $\mathbf{f} = \mathbf{u} \odot \mathbf{u}/2$ is the inviscid flux (and \odot denotes the elementwise Hadamard product), and BC represents the boundary conditions. The operator $\mathbf{P}^{-1}\tilde{\mathbf{D}}_p^T(\cdot)\tilde{\mathbf{D}}_p$ represents the narrow stencil form of the $(2p)$ th derivative (Mattsson *et al.* 2004). The matrix

$\mathbf{P} = \mathbf{P}^T > 0$ is a norm and if $\mathbf{Q} + \mathbf{Q}^T = \text{diag}(-1, 0, \dots, 0, 1)$ the method satisfies the summation-by-parts (SBP) condition (Strand 1994). That Eq. (3.1) applies to non-SBP methods requires a little tedious algebra but has been shown in Abbas *et al.* (2009) for finite-volume schemes and by Fisher *et al.* (2011) for WENO-like schemes. We further restrict ourselves to the simultaneous-approximation-term approach (Svärd & Nordström 2014) to boundary condition implementation that yields energy stable schemes so that

$$\text{BC} = -\mathbf{P}^{-1}\mathbf{E}_0u_0^+(u_0 - g_0) + \mathbf{P}^{-1}\mathbf{E}_Nu_N^-(u_N - g_N), \quad (3.2)$$

where $\mathbf{u} = [u_0, u_1, \dots, u_N]^T$, $u_0^+ = (u_0 + |u_0|)/2$, $u_N^- = (u_N - |u_N|)/2$, and \mathbf{E}_0 and \mathbf{E}_N are equal to zero except that the $(1, 1)$ and $(N + 1, N + 1)$ elements, respectively, are equal to one. The g_0 and g_N values represent the left and right boundary data, respectively. Specification of \mathbf{D}_1 , \mathbf{D}_p , and Φ uniquely defines the numerical method. The finite-volume methods (Lax-Friedrichs and MUSCL, (Leveque 2002)), WENO (the original of Jiang & Shu (1996) and an energy-stable variant ESWENO (Fisher *et al.* 2011)) and the LAD method of Kawai & Lele (2008) were implemented using the `jax` (Bradbury *et al.* 2018) Python toolkit to enable autodifferentiation for computing discrete adjoints.

3.1. Example forward and adjoint solutions to the Riemann problem

The analytical solutions to the forward and adjoint Riemann problems given in Section 2 serve as the standard against which numerical solutions are compared. The particular values of $g_0 = u_L = 1$, $u_R = 0$, $x_0 = 0$, $-a = b = 1$, and $u^* \equiv 0$ define the optimization problem, of which only one forward calculation and one adjoint calculation are performed. (Further iterations would be needed if optimization was the goal.) We choose to evaluate the methods by examining the adjoint solution at $t = 0$, which should approximate the analytical solution of

$$p(x, 0) = \begin{cases} 1 & x < -1/2 \\ 1/2 & -1/2 < x < 1/2 \\ 0 & x > 1/2. \end{cases} \quad (3.3)$$

Figure 2 shows typical results for the four schemes indicated. The key feature of Figure 2 is the plateau value of the adjoint solution near the origin $x = 0$. The analytical solution of $1/2$ is well approximated by the Lax-Friedrichs and LAD methods and not by MUSCL or WENO. It can be numerically demonstrated that neither grid refinement nor time-step refinement will induce the MUSCL or WENO method to converge to the analytical; there is a fundamental difference with the analytical solution. Although we do not show it here, ESWENO performed similarly to MUSCL and WENO and was unable to converge the analytical adjoint solution.

4. Conditions for a convergent adjoint method

The results of the previous section demonstrate that some numerical methods produce discrete adjoints that converge to the analytical solution (Lax-Friedrichs and LAD) and some do not (MUSCL, WENO, and ESWENO). It is important to remember that all five methods were developed to produce accurate approximations of the forward problem with discontinuities, and the literature shows that their use is widespread. To connect the methods with their discrete adjoint properties, we appeal to their description in Eq. (3.1) and derive the corresponding adjoint method-of-lines equation. To do so, we define the

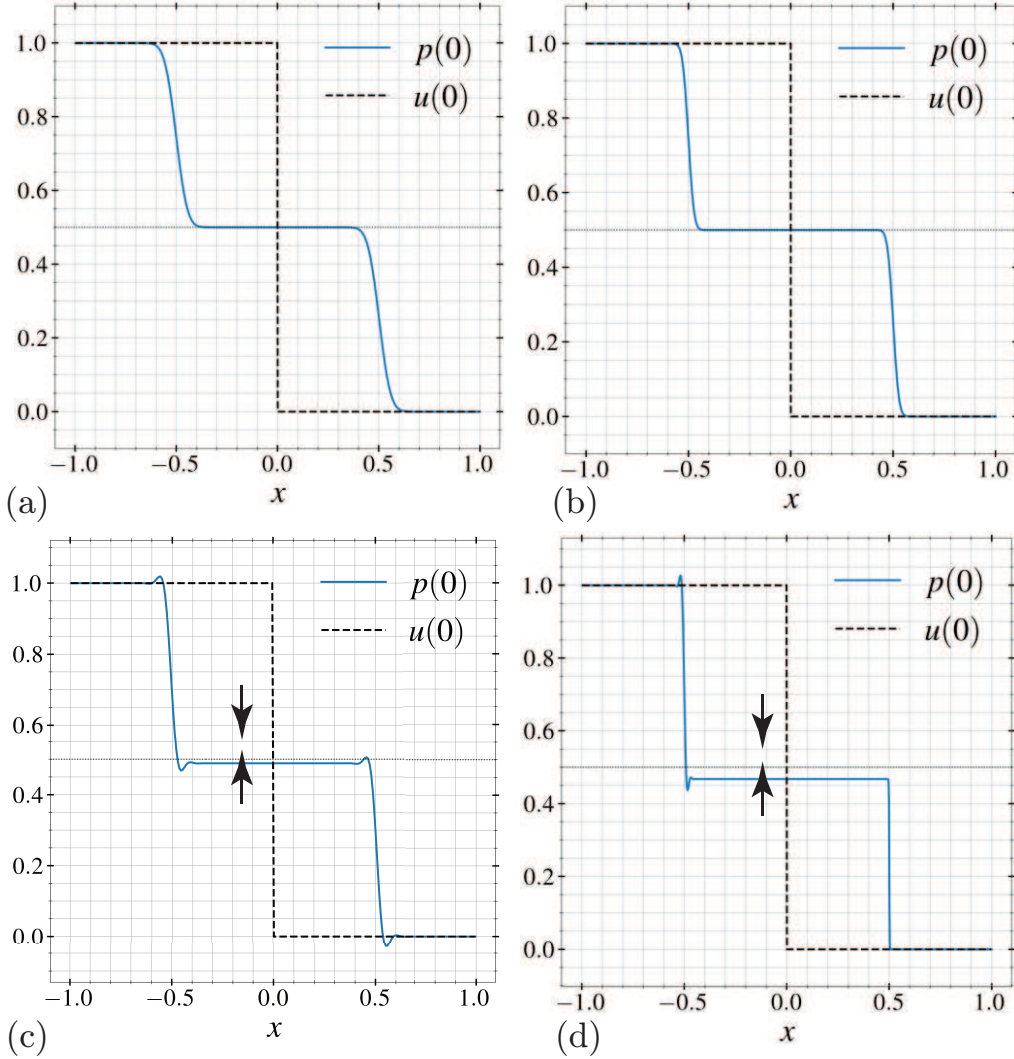


FIGURE 2. Adjoint solutions $p(x,0)$ for several numerical methods: (a) Lax-Friedrichs, (b) LAD of Kawai & Lele (2008), (c) MUSCL of Abbas *et al.* (2009), and (d) WENO32 of Jiang & Shu (1996).

P-based inner product $\langle \mathbf{a}, \mathbf{b} \rangle_{\mathbf{P}} = \mathbf{a}^T \mathbf{P} \mathbf{b}$ and the Lagrangian

$$\mathcal{L}[\mathbf{u}, \mathbf{p}] = \mathcal{J}[\mathbf{u}] - \left\langle \mathbf{p}, \frac{d\mathbf{u}}{dt} + \mathbf{D}_1[\mathbf{u}]\mathbf{f} - \mathbf{P}^{-1} \tilde{\mathbf{D}}_p^T \Phi[\mathbf{u}] \tilde{\mathbf{D}}_p \mathbf{u} + \text{BC} \right\rangle_{\mathbf{P}} \quad (4.1)$$

in the usual way. When the variations $\tilde{\mathbf{u}}$ and $\tilde{\mathbf{p}}$ are added to their base functions \mathbf{u} and \mathbf{p} , the adjoint equations arise by requiring that the first variation of \mathcal{L} , defined as $\mathcal{L}[\mathbf{u} + \tilde{\mathbf{u}}, \mathbf{p} + \tilde{\mathbf{p}}] - \mathcal{L}[\mathbf{u}, \mathbf{p}]$, be zero for all possible variations $(\tilde{\mathbf{u}}, \tilde{\mathbf{p}})$. The end result of the algebra is the method-of-lines scheme

$$-\frac{d\mathbf{p}}{dt} - \mathbf{u} \odot \mathbf{D}_1[\mathbf{u}]\mathbf{p} = \mathbf{P}^{-1} \tilde{\mathbf{D}}_p^T \Phi[\mathbf{u}] \tilde{\mathbf{D}}_p \mathbf{p} + \text{BC}^\dagger + G'(\mathbf{u}; \mathbf{u}^*) + \mathbf{S}[\mathbf{u}]\mathbf{p}, \quad (4.2)$$

where it is understood that \mathbf{u} satisfies the forward equation (Eq.(3.1)), BC^\dagger are the adjoint boundary conditions, and $\mathbf{S}[\mathbf{u}]$ is a source term that will be discussed in the subsequent paragraphs.

The contributions to \mathbf{S} arise from the nonlinearities in the operators $\text{D}_1[\mathbf{u}]$ (as in WENO and ESWENO) and from those in $\Phi[\mathbf{u}]$ for MUSCL and LAD. In the former case, algebra shows that \mathbf{S} has a contribution of the form

$$\mathbf{P}^{-1}\tilde{\mathbf{Q}}[\mathbf{u}]\mathbf{p},$$

where $\tilde{\mathbf{Q}}[\mathbf{u}]$ is proportional to the variation in the matrix \mathbf{Q} with respect to the solution \mathbf{u} , with the matrix constant of proportionality depending on the specifics of the scheme. Important to the adjoint is the fact that the variation of \mathbf{Q} is not smooth with respect to \mathbf{u} because of the stencil-switching functions used to define WENO and ESWENO (see, for example, Jiang & Shu (1996)) which, by construction, are active in the vicinity of the shock. Thus the source term \mathbf{S} is non-zero in the vicinity of the shock and its value does not diminish with increasing grid resolution but, instead, occupies a smaller spatial support. A linear scheme, in contrast, has $\tilde{\mathbf{Q}} \equiv 0$.

In the latter case, for MUSCL and LAD methods, the source term is proportional to the variation of $\Phi[\mathbf{u}]$. For LAD methods of the type of Kawai & Lele (2008), which are composite differentiable functions of derivatives of the solutions, the variation of Φ with \mathbf{u} is smooth and can be related to $d\Phi[\mathbf{u}]/d\mathbf{u}$. Note that this form of \mathbf{S} implies that the adjoint system is not necessarily energy stable and motivates the concept of nonlinear sensitivity equations (Nordström 2022).

For MUSCL schemes, on the other hand, the elements of $\Phi[\mathbf{u}]$ are computed on the basis of the bounded variation of the solution between adjacent cells. For example, Abbas *et al.* (2009) give the i th diagonal element of Φ as

$$\frac{1}{2} \left\{ |\{\{u\}\}_i| (1 - \phi_i/2 - \psi_{i+1}/2) + u_{i+1/2}^R \psi_{i+1}/2 - u_{i+1/2}^L \phi_i/2 \right\},$$

where $u_{i+1/2}^L = u_i + \phi(r_i)(u_{i+1} - u_i)/2$ is the MUSCL-estimated state using left-of-face data and $\phi(r_i)$ is the flux limiter function dependent on $r_i = (u_i - u_{i-1})/(u_{i+1} - u_i)$. The MUSCL-estimated state using right-of-face data is $u_{i+1/2}^R = u_{i+1} - \phi(r_{i+1})(u_{i+2} - u_{i+1})/2$. The slope limiters ϕ and ψ are non-smooth by construction for some values of r , with at least one slope discontinuity at $r = 0$ and one or two more at $r = 1$ and $r = 2$, depending on the specific limiter. When the variation of Φ is evaluated, these jumps in ϕ' appear as additional source terms in \mathbf{S} with magnitudes that do not diminish with increasing grid resolution; instead, they become more spatially compact, as in the case of WENO and ESWENO.

5. Conclusions

The study of discrete adjoint solutions to the Riemann problem of the nonlinear inviscid Burgers equation has been conducted, with an emphasis on the convergence of the numerical adjoint solution to its analytical companion. Using a method-of-lines formulation with potentially nonlinear operators to represent commonly used shock capturing methods of MUSCL and WENO (and their variants), it is shown that the method-of-lines adjoint equation contains anomalous source terms with magnitudes that are independent of the grid spacing and proportional to the underlying stencil-switching or slope limit

discontinuities. Only the localized artificial diffusivity class of methods was found to yield meaningful adjoint solutions.

Acknowledgments

D. J. B. is grateful for the contributions of Mr. Sandeep Murthy of the University of Illinois at Urbana-Champaign and for thoughtful discussions with Professor Spencer Bryngelson of Georgia Tech.

REFERENCES

- ABBAS, Q., DER WEIDE, E. V. & NORDSTRÖM, J. 2009 Accurate and stable calculations involving shocks using a new hybrid scheme. *AIAA Paper* 2009-3985.
- BOUCHUT, F. & JAMES, F. 1998 One-dimensional transport equations with discontinuous coefficients. *Nonlinear Anal.* **32** (7), 891–933.
- BRADBURY, J., FROSTIG, R., HAWKINS, P., JOHNSON, M. J., LEARY, C., MACLAURIN, D., NECULA, G., PASZKE, A., VANDERPLAS, J., WANDERMAN-MILNE, S. & ZHANG, Q. 2018 JAX: composable transformations of Python+NumPy programs.
- COOK, D. A. & NICHOLS, J. W. 2022 Free stream receptivity of a hypersonic blunt cone using input–output analysis and a shock-kinematic boundary condition. *Theor. Comput. Fluid Dyn.*
- FISHER, T. C., CARPENTER, M. H., YAMALEEV, N. K. & FRANKEL, S. H. 2011 Boundary closures for fourth-order energy stable weighted essentially non-oscillatory finite-difference schemes. *J. Comput. Phys.* **230**, 3727–3752.
- GILES, M. B. & PIERCE, N. 2001 Analytic adjoint solutions for the quasi-one-dimensional Euler equations. *J. Fluid Mech.* **426**, 327–345.
- GILES, M. B. & ULBRICH, S. 2010a Convergence of linearized and adjoint approximations for discontinuous solutions of conservation laws. Part 1: Adjoining approximations and extensions. *SIAM J. Numer. Anal.* **48**, 905–921.
- GILES, M. B. & ULBRICH, S. 2010b Convergence of linearized and adjoint approximations for discontinuous solutions of conservation laws. Part 1: Linearized approximations and linearized output functionals. *SIAM J. Numer. Anal.* **48**, 882–904.
- JAMESON, A. 1988 Aerodynamic design via control theory. *J. Sci. Comput.* **3**, 233–260.
- JIANG, G.-S. & SHU, C.-W. 1996 Efficient implementation of weighted ENO schemes. *J. Comput. Phys.* **126**, 202–228.
- JORDAN, P. & COLONIUS, T. 2013 Wave packets and turbulent jet noise. *Ann. Rev. Fluid Mech.* **45**, 173–195.
- KARP, M., FLINT, T. & HACK, M. J. P. 2020 Global stability analysis of supersonic jets. *AIAA Paper* 2020-1248.
- KAWAI, S. & LELE, S. K. 2008 Localized artificial diffusivity scheme for discontinuity capturing on curvilinear meshes. *J. Comput. Phys.* **227**, 9498–9526.
- KIM, J., BODONY, D. J. & FREUND, J. B. 2014 Adjoint-based control of loud events in a turbulent jet. *J. Fluid Mech.* **741**, 28–59.
- LEVEQUE, R. J. 2002 *Finite Volume Methods for Hyperbolic Problems*. Cambridge Univ. Press.
- LIU, J., CORRIGAN, A. & KAILASANATH, K. 2016a Effects of temperature on noise generation in supersonic jets. *AIAA Paper* 2016-2937.
- LIU, J., CORRIGAN, A., KAILASANATH, K. & TAYLOR, B. 2016b Impact of the specific

- heat ratio on noise generation in a high-temperature supersonic jet. *AIAA Paper* 2016-2125.
- MATSSON, K., SVÄRD, M. & NORDSTRÖM, J. 2004 Stable and accurate artificial dissipation. *J. Sci. Comput.* **21** (1), 57–79.
- NATARAJAN, M., FREUND, J. B. & BODONY, D. J. 2018 Global mode-based control of laminar and turbulent high-speed jets. *C. R. Mecanique* **346** (10), 978–996.
- NORDSTRÖM, J. 2022 Nonlinear and linearised primal and dual initial boundary value problems: When are they bounded? How are they connected? *J. Comput. Phys.* **455**, 111001.
- SCHLINKER, R. H., SIMONICH, J. C., SHANNON, D. W., REBA, R. A., COLONIUS, T., GUDMUNDSSON, K. & LADEINDE, F. 2009 Supersonic jet noise from round and chevron nozzles: experimental studies. *AIAA Paper* 2009-3257.
- STRAND, B. 1994 Summation by parts for finite difference approximations for d/dx . *J. Comput. Phys.* **110**, 47–67.
- SUZUKI, T. & COLONIUS, T. 2006 Instability waves in a subsonic round jet detected using a near-field phased microphone array. *J. Fluid Mech.* **565**, 197–226.
- SVÄRD, M. & NORDSTRÖM, J. 2014 Review of summation-by-parts schemes for initial-boundary-value problems. *J. Comput. Phys.* **268**, 17–38.
- WALTON, J. W. & BURCHAM, F. W. 1986 Exhaust-gas pressure and temperature survey of F404-GE-400 turbofan engine. Tech. Memo. 88273, National Aeronautics and Space Administration.